ELSEVIER

Journal of Molecular Catalysis A: Chemical 167 (2001) 91–99

JOURNAL OF MOLECULAR CATALYSIS A: CHEMICAL

www.elsevier.com/locate/molcata

Synthesis, characterization and catalytic properties of $Pt/CeO_2–Al_2O_3$ and $Pt/La_2O_3–Al_2O_3$ sol–gel derived catalysts

A. Vazquez [a], T. Lopez [b], R. Gomez [a,b,*], X. Bokhimi [c]

[a] *Instituto Mexicano del Petroleo, Eje Central Lazaro Cardenas No. 152, Mexico 07000, D.F., Mexico*
[b] *Department of Chemistry, Universidad Autonoma Metroplitana-Iztapalapa, P.O. Box 55-534, Mexico 9340, D.F., Mexico*
[c] *UNAM Instituto de Fisica, Ciudad Universitaria, Mexico 09000, D.F., Mexico*

Received 6 April 2000

Abstract

Platinum supported on $La_2O_3–Al_2O_3$ and $CeO_2–Al_2O_3$ were prepared by the sol–gel method. High specific surface areas between 572–418 m^2/g were obtained. FTIR-pyridine absorption band proved the formation of Lewis sites with comparable intensity in the supports. The stabilization of the γ-Al_2O_3 in the $La_2O_3–Al_2O_3$ support was observed by X-ray diffraction when the sample was calcined at 1100°C, while segregation of CeO_2 was observed at such temperature in the $CeO_2–Al_2O_3$ preparation. The formation of Al^V and Al^{VI} coordinated aluminum was observed by MAS-NMR ^{27}Al spectra in La doped-alumina. In the Ce doped-sample only Al^{VI} coordination was identified. Propene and acetone were the products in the *iso*-propanol decomposition over $CeO_2–Al_2O_3$, meanwhile, for the $La_2O_3–Al_2O_3$ support only propene was obtained. The platinum (0.5 wt.%) particle size distribution as determined by electron microscopy showed very small particles <1.0 nm. On the other hand, in the *n*-heptane dehydrocyclization the activity and selectivity to toluene of the $Pt/La_2O_3–Al_2O_3$ catalyst was found bigger than those of $Pt/CeO_2–Al_2O_3$ catalyst. It is proposed that doped-alumina prepared by the sol–gel method has structural defects which induce modification in the metal activity.

Keywords: Sol–gel catalysts; Platinum lanthanum–alumina; Platinum cerium–alumina; MAS-NMR sol–gel catalysts; Acidity sol–gel catalysts

1. Introduction

The preparation of metal supported catalysts by the sol–gel method has been demonstrated to be useful for a large number of applications [1]. For example, highly resistant catalysts to sintering or poisoning by coke and sulfur were prepared by adding ruthenium [2–4], palladium [5–8] or platinum precursors to silica gel [9–13]. In reforming $Pt–Sn/Al_2O_3$ catalysts prepared by co-gelling aluminum tri-*sec*-butoxide and tetrabutyl tin, efficient catalysts for the *n*-heptane dehydrocyclization were obtained [14–17]. Bimetallic $Pd–Co/SiO_2$ catalysts prepared by the sol–gel method have been reported as selective catalysts for the hydrogenation of CO [18,19]. The gas exhaust catalytic converter reactions like carbon monoxide oxidation was carried out in high metal sintering resistance Pt/TiO_2 sol–gel catalysts [20]. The non-selective catalytic reduction of NO by CO on Pt/Al_2O_3 and Rh/Al_2O_3 and $Pd/La_2O_3–Al_2O_3$ prepared by the sol–gel method have also been reported [21–23]. Moreover, Rh/ZrO_2 catalysts show high activity for the combustion of

* Corresponding author. Tel.: +52-5804-5668; fax: +52-5804-4666.
E-mail address: gomr@xanum.uam.mx (R. Gomez).

1381-1169/01/$ – see front matter
PII: S1381-1169(00)00495-7

methane [24]. The also called one-step preparation of supported metal catalysts improved the catalytic properties of the metallic phase [25,26]. Little attention, however, has been given in the preparation of metal supported sol–gel catalysts in which modifications to the support are induced in the preparation step. Most papers concerning alumina support modifications are related to the alumina mixed oxides. The synthesis by the sol–gel method of alumina–zirconia, alumina–magnesia or alumina–silica as supports have been recently reported [27–29].

Without doubt, alumina is the support most widely used in metal-supported catalysts and because of its importance, alumina is the support largely used in gas exhaust catalytic converters. In the three way catalysts, the alumina contains CeO_2 as support additive. The role of the CeO_2 in the reduction of CO or NO emissions is confined to an additional oxygen source [30–32]. The effect of ceria in the activity of the noble metals, however, has not been clearly defined and metal–Ce interactions are given to explain the increased activity of the metal [33,34]. The preparation of CeO_2–Al_2O_3 or La_2O_3–Al_2O_3 supports currently is done by the impregnation of the support with the rare earth precursors. The effect of the lanthanides on the catalytic properties is then confined to alumina surface effects [35].

In the present work with the aim to induce textural and structural effects in alumina, alumina-gel was prepared by adding to aluminum tri-*sec*-butoxide cerium or lanthanum nitrate. The gelled CeO_2–Al_2O_3 and La_2O_3–Al_2O_3 supports were then impregnated with hexachloroplatinic acid to obtain the metal/doped-alumina catalysts (sol–gel method). In such a way, the La_2O_3 or CeO_2 role is not limited to surface effects, since Ce or La could be incorporated in the alumina network [36–38]. Structural defects as well as a good thermal stabilization of the alumina is expected, depending on the gelling conditions and rare earth metal oxide precursors. The characterization of the obtained sol–gel supports and platinum supported catalysts were done by means of FTIR-pyridine absorption spectroscopy, X-ray diffraction, MAS-NMR spectroscopy, and by the catalytic test in the *iso*-propanol dehydration (support acidity), cyclohexane dehydrogenation (metallic dispersion), and *n*-heptane aromatization (bi-functional reaction).

2. Experimental

2.1. Catalysts preparation

Sol–gel Al_2O_3 reference support was prepared by mixing aluminum tri-*sec*-butoxide (Aldrich 97%), $Al(OC_4H_9sec)_3$ (0.207 mol), in 6.5 mol of absolute ethanol (Merck) at 60°C. The reactants were maintained under constant stirring and refluxing. Distilled water (2.94 mol) was added to the mixture and the gelling reaction was completed. Thereafter, the gel was dried in air at 70°C for 24 h (fresh sample). For characterization various thermal treatments were done at the temperatures given in the text.

Sol–gel La_2O_3/Al_2O_3 support were prepared by refluxing aluminum tri-*sec*-butoxide (Aldrich 97%), $Al(OC_4H_9sec)_3$ (0.207 mol), in 6.5 mol of absolute ethanol (Merck) at 60°C. Afterwards 2.94 mol of distilled water containing the appropriated lanthanum nitrate concentration was added to the aluminum alkoxide solution. The gelling reaction was accomplished after 1 h under reflux. The gel was then dried in air at 70°C. For the synthesis of CeO_2–Al_2O_3 support, the procedure used to prepare La_2O_3–Al_2O_3 samples was accomplished adding in this case cerium nitrate as cerium precursor. The La_2O_3 and CeO_2 content in alumina was 5 wt.%.

The Pt/La_2O_3–Al_2O_3 and Pt/CeO_2–Al_2O_3 catalysts were prepared by impregnation of the sol–gel supports (calcined at 500°C in air for 2 h) with an aqueous solution containing the desired amount of hexachloroplatinic acid (K&K) to obtain 0.5 wt.% of Pt. After impregnation the catalysts were dried in air at 120°C for 12 and then reduced in hydrogen flow for 4 h at 500°C.

2.2. Specific surface area determination

The specific surface area, pore volume and mean pore diameter were measured with an ASAP 2000 Micromerictics analyzer, the data were obtained from the nitrogen adsorption isotherm of the 500°C calcined supports. The specific area was calculated from the BET equation and the mean pore size diameter from the BJH method. Before the measurements the samples were desorbed at 400°C for 2 h.

2.3. FTIR-pyridine adsorption

The calcined supports were characterized in situ with a Nicolet 170 SX spectrometer using a vacuum cell (1×10^{-6} Torr) in which atmosphere and temperature are controlled. Self support samples were prepared by pressing the solid until transparency was obtained. The acid sites were characterized exposing the pellet to pyridine which is introducing in the cell through a saturator with flowing nitrogen at room temperature. Excess pyridine was removed under vacuum and the temperature of the cell was then raised to 100°C and after to 200°C. The pyridine absorption spectra were obtained at these desorption temperatures.

2.4. X-ray diffraction analysis

In samples annealed at different temperatures, the crystalline or amorphous structure was obtained at room temperature by using X-ray powder diffraction (Siemens 500-D). The reflection diffractometer used a Cu Kα radiation, and had a graphite monochromator in the secondary bean. Intensity data were measured by step scanning in the 2θ ranges between 2 and 110° and between 2 and 70°, with a 2θ step of 0.02° and a measuring time of 1 s per point.

2.5. MAS-NMR spectroscopy

Powder samples were analyzed in a Brucker ASX-300 NMR spectrometer. The study was done with the ^{27}Al isotope at a frequency of 78.21 MHz with a spinning speed of 12 kHz. Chemical shifts were referred to aluminum in $Al(H_2O)_6^{3+}$ ion.

2.6. Catalytic test

iso-Propanol decomposition activity was performed in a flowing microreactor linked with a gas-chromatograph. *iso*-Propanol (Aldrich 99.9%) was contained in a double H saturator embedded in a recipient with a mixture of ice and water. Saturated nitrogen with *iso*-propanol was passed through the reactor. The partial pressure of the reactant was 22.4 Torr and the reaction temperature 200°C. The cyclohexane dehydrogenation was performed using the same reactant system described for *iso*-propanol decomposition. The reaction conditions were: gas flow nitrogen, cyclohexane partial pressure 29 Torr, reaction temperature 200°C. For the *n*-heptane dehydrocyclization, the catalytic activity test conditions were: gas flow hydrogen; *n*-heptane partial pressure 11 Torr; reaction temperature 500°C. Before activity evaluation (50 mg), the samples were reactivated in the glass reactor (2 ml) with gas flow (nitrogen or hydrogen) for 2 h at 400°C.

3. Results

3.1. La_2O_3–Al_2O_3 and CeO_2–Al_2O_3 characterization

Data on the specific surface area, mean pore size diameter and pore volume are shown in Table 1. The Al_2O_3 sample shows a large specific surface area (572 m^2/g) and a pore size diameter of 7.0 nm. In La_2O_3 or CeO_2, doped-alumina the BET areas were 459 and 418 m^2/g and the pore size diameter 5.5 and 6.0, respectively. A BET area diminution around 20–30% for doped-alumina was then obtained. Typical isotherms and pore size distribution for alumina and doped-alumina are shown in Figs. 1 and 2, respectively.

FTIR-pyridine adsorption was used to determine the type of acid sites on supports calcined at 500°C. In the infrared spectrum of pyridine absorption on acid catalysts the bands observed around 1590, 1490 and 1450 cm^{-1} are assigned to the different modes of vibration of the pyridine adsorbed on Lewis sites [39]. The absorption bands of Fig. 3 correspond then to supports showing Lewis acidity. The relative intensity between these bands differs slightly in alumina or doped-aluminas. Note that the pyridine absorption band around 1540 cm^{-1} assigned to Bronsted acid sites [40] is not observed in the sol–gel alumina and doped samples.

Amorphous alumina was observed in the X-ray diffraction pattern when samples were thermally treated at temperatures of 500°C. When the samples were treated at 1000°C low crystalline γ-Al_2O_3 formation is observed. However, in samples annealed at 1100°C, the formation of highly crystalline α-Al_2O_3 is observed for alumina sol–gel (Fig. 4). For La_2O_3 doped-alumina, the γ-Al_2O_3 crystalline phase remains

Table 1
Specific surface area, mean pore diameter and pore volume of Al_2O_3, doped La_2O_3–Al_2O_3 and CeO_2–Al_2O_3 sol–gel prepared supports

Support[a]	BET area (m^2/g)	Pore diameter (nm)	Pore volume (cm^3/g)
Al_2O_3	572	7.0	0.88
La_2O_3–Al_2O_3	459	5.3	0.61
CeO_2–Al_2O_3	418	6.0	0.56

[a] Calcined in air at 500°C for 4 h.

present even after thermal treatment at 1100°C. The X-ray diffraction pattern for the CeO_2 doped-alumina is different, after thermal treatment at 1000°C, the γ-Al_2O_3 phase is still observed. However, if the sample is calcined at 1100°C, the transformation to α-Al_2O_3 and cerianite can be observed. The different behavior shown by the ceria doped-alumina is indicative that possible segregation of ceria occurs in the sample.

MAS-NMR ^{27}Al spectra of the samples treated at 1100°C are shown in Fig. 5. ^{27}Al RMN signals are reported between 55 and 70 ppm for tetrahedral aluminum Al^{IV}, around 25–30 ppm for a pentacoordinated Al^{V} (or deformed tetrahedral aluminum), and at 0–11 ppm for octahedrally coordinated Al^{VI} [29,41]. Alumina and CeO_2–Al_2O_3 samples show the corresponding peak for octahedrally coordinated aluminum, while in La_2O_3–Al_2O_3 in addition to the octahedral aluminum a signal assigned to deformed tetrahedral coordination is observed.

iso-Propanol decomposition gives propene, acetone and *iso*-propylether as main products and the reaction is reported as a test reaction to determine the acidic–basic character of solids [39]. Comparable activities were obtained in doped and non-doped alumina (Table 2). However, the selectivity pattern notably differs between them. In Al_2O_3 support propene (87%)

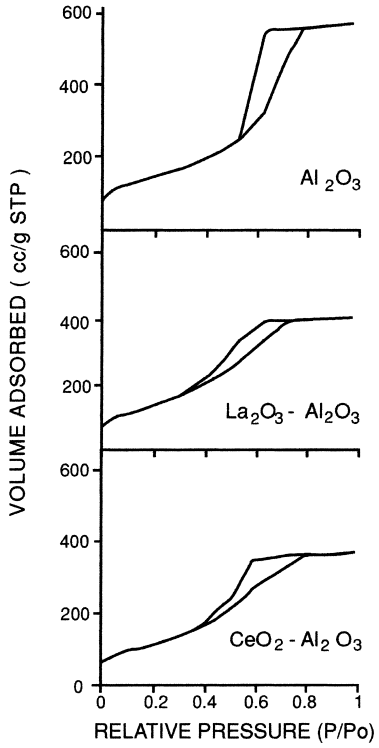

Fig. 1. Nitrogen adsorption isotherms of Al_2O_3, La_2O_3–Al_2O_3 and CeO_2–Al_2O_3 sol–gel prepared supports.

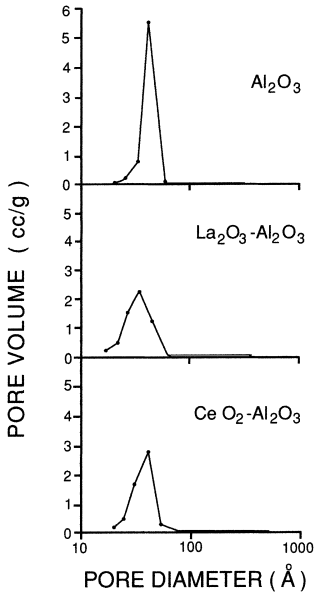

Fig. 2. Pore size distribution of Al_2O_3, La_2O_3–Al_2O_3 and CeO_2–Al_2O_3 sol–gel prepared supports.

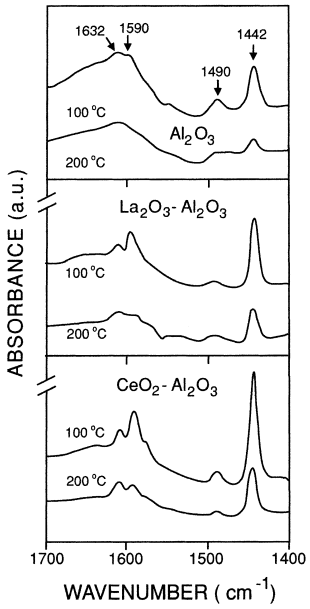

Fig. 3. FTIR-pyridine adsorption spectra of Al_2O_3, La_2O_3–Al_2O_3 and CeO_2–Al_2O_3 sol–gel prepared supports.

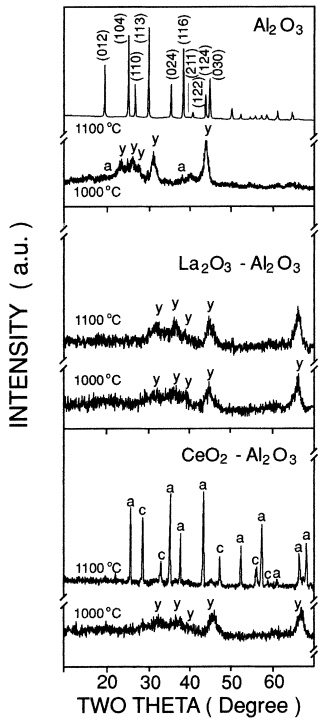

Fig. 4. X-ray diffraction spectra of Al_2O_3, La_2O_3–Al_2O_3 and CeO_2–Al_2O_3 sol–gel prepared supports.

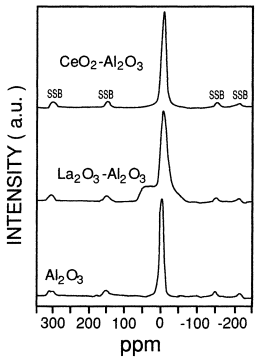

Fig. 5. MAS-NMR spectra of Al_2O_3, La_2O_3–Al_2O_3 and CeO_2–Al_2O_3 sol–gel prepared supports.

and *iso*-propylether (13%) were obtained. On the other hand, in ceria–alumina propene (65%) and acetone were the products, while for La_2O_3–Al_2O_3 alumina the only product was propene (100%). The total rate is related to the total acidity of the catalysts while the selectivity depends of its relative strength [39]. These results are indicative that in alumina and doped-alumina sol–gel samples, the total acidity is comparable, while different acid site strength distribution is expected.

3.2. *Pt/La_2O_3–Al_2O_3 and Pt/CeO_2–Al_2O_3 characterization*

The metallic phase of the Pt supported on La and Ce doped-alumina was characterized by determining its catalytic properties. In Table 3, the activity of the catalysts for the cyclohexane dehydrogenation is reported. The Pt/Al_2O_3 reference catalyst showed an initial activity twice that shown by the Pt/La_2O_3–Al_2O_3 and Pt/CeO_2–Al_2O_3 catalysts. This constitutes a support or metallic dispersion effect in activity. In Table 3, the

Table 2
Activity and selectivity for the *iso*-propanol dehydration on Al_2O_3, doped La_2O_3–Al_2O_3 and CeO_2–Al_2O_3 sol–gel prepared supports

Support[a]	Specific rate ($\times 10^7$) (mol/g s)	Selectivity (%)		
		Propene	Acetone	*iso*-Propyl-ether
Al_2O_3	1.18	87	–	13
La_2O_3–Al_2O_3	1.40	100	–	–
CeO_2–Al_2O_3	1.12	65	35	

[a] Calcined in air at 500°C for 4 h.

Table 3
Cyclohexane dehydrogenation on Pt/Al_2O_3, Pt/La_2O_3–Al_2O_3 and Pt/CeO_2–Al_2O_3 sol–gel prepared catalysts

Catalysts	Conversion (%)	$k_d \times 10^3$ min[a]
Pt/Al_2O_3	20	2.3
Pt/La_2O_3	10	0.2
Pt/CeO_2	10	0.7

[a] Constant deactivation.

deactivation constant for the reaction is reported. It is calculated from the deactivation rate law $C_0/C = 1 + k_d t$. The relative deactivation constant was obtained by plotting the reciprocal of conversion as a function of time. The appropriate use of this equation to calculate the deactivation constant is reported and discussed in previous work [2]. A relative deactivation constant of 2.3 was obtained for the Pt/Al_2O_3, while small values of 0.2 and 0.7 were obtained for the Pt/La_2O_3–Al_2O_3 and Pt/CeO_2–Al_2O_3 catalysts, respectively. These results show that in platinum doped alumina the deactivation is strongly inhibited if compared with non-doped alumina.

The *n*-heptane transformation is an activity test indicative of the performance of catalysts in naftha reforming process. In Table 4, the activity and the selectivity for the *n*-heptane transformation in the platinum supported catalysts are reported. High activities (38 and 34%) for the platinum supported in La and Ce doped-alumina are observed, while the activity of Pt supported on non-doped alumina is 16%. Certainly, the support acidity plays an important role in the *n*-heptane transformation. The selectivity pattern for the reaction is reported as a useful value to compare catalyst behaviors. The products in *n*-heptane reforming are C_1–C_4, C_5–C_7 fractions and toluene. It can be seen in Table 4, that the toluene/C_1–C_4 ratio are 1.08, 1.26 and 2.08 for Pt/Al_2O_3, Pt/CeO_2-Al_2O_3 and Pt/La_2O_3–Al_2O_3, respectively. A similar ratio

Table 4
n-Heptane dehydrocyclization on Pt/Al_2O_3, Pt/La_2O_3–Al_2O_3 and Pt/CeO_2–Al_2O_3 sol–gel prepared catalysts

Catalysts	Conversion (%)	Selectivity (mol%)			
		[(a)]C_1–C_4	[(b)]C_5–C_7	Toluene	*a*/*b*
Pt/Al_2O_3	16	35	27	38	1.08
Pt/La_2O_3–Al_2O_3	48	24	26	50	2.08
Pt/CeO_2–Al_2O_3	34	30	32	38	1.28

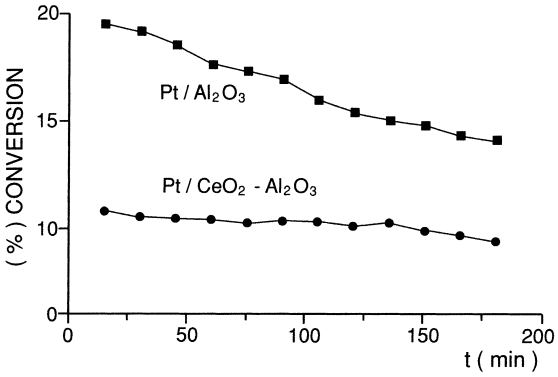

Fig. 6. Catalysts evolution on function of time of Pt/Al_2O_3 and Pt/CeO_2–Al_2O_3 sol–gel prepared supports during the cyclohexane dehydrogenation.

toluene/C_5–C_7 trend was also found on the catalysts. These results show that the Pt/La_2O_3–Al_2O_3 catalyst has the better activity and selectivity to the desired products on the *n*-heptane transformation.

4. Discussion

The adsorption isotherms of the three samples shown in Fig. 1 can be classified as similar, i.e. they each show a hysteresis loop. The lowest BET areas of the doped-aluminas (459 and 418 m^2/g) compared with the non-doped one (572 m^2/g) are certainly due to the addition of cerium or lanthanum nitrate to the aluminum alkoxide during gellation. Using sol–gel synthesis, the incorporation of lanthanum or cerium into the alumina network can be expected and hence a diminution of the pore size diameter can occur. In Fig. 2, a narrow pore size mesoporous distribution is observed for alumina (mean pore diameter 7.0 nm), while a broad pore size distribution and mean pore size diameters of 5.3 and 6.0 nm is obtained for the La_2O_3–Al_2O_3 and CeO_2–Al_2O_3 supports, respectively. The lowest specific surface areas of the doped-aluminas may be a side effect due of the diminution of the pore size diameter. However, it is not possible with only this information to discriminate between an effect due to the incorporation of the rare earth oxides into the alumina network or an effect due to the deposit of La_2O_3 or CeO_2 into the pore.

To discriminate between such effects X-ray diffraction studies were carried out. The spectra obtained for

alumina and doped-aluminas annealed to 1000°C correspond to γ-Al_2O_3 structure (Fig. 4). When the samples were treated at 1100°C, the crystalline structure of alumina reference was transformed in α-alumina, while the CeO_2–Al_2O_3 shows two crystalline structures α-Al_2O_3 and a cerianite. On the other hand, we can see that for La_2O_3–Al_2O_3, γ-Al_2O_3 phase is the only structure present. These results suggest that in preparing the alumina by the sol–gel method, the γ-Al_2O_3 phase is stable up to 1000°C. The stabilization of the γ-Al_2O_3 phase at such temperature is not usual, since frequently a mixture of the γ-Al_2O_3 and α-Al_2O_3 phases containing important percentage of the latter is observed when the alumina was prepared from soluble salts. The formation of the α-Al_2O_3 and cerianite structures in the CeO_2–Al_2O_3 support after treatment at 1100°C is indicative that in this sample a segregation of ceria is occurring. Ceria stabilizes the γ-Al_2O_3 up to 1000°C, afterwards the ceria goes out of the alumina structure and then the α-Al_2O_3 phase is formed. La_2O_3 segregation phenomena is not observed in the La_2O_3–Al_2O_3 sample. The lanthanide stabilizes the γ-Al_2O_3 crystalline phase even after thermal treatment at 1100°C [38].

Since in the three samples treated at 500°C incipient γ-Al_2O_3 crystalline phase is observed by X-ray diffraction, it is proposed that during the gellation of alumina the rare earth oxides were incorporated in the alumina network. The amount of the oxide incorporate is difficult to evaluate. However, the probability that La_2O_3 was incorporate in a larger quantity than cerium is supported from the X-ray diffraction data. Unfortunately, the X-ray diffraction technique is not sensitive enough to identify high dispersed La_2O_3 on the alumina surface.

To identify La in the alumina network, the study of the Al environment by MAS-NMR was made. The spectra of samples treated at 1100°C are shown in Fig. 5. The spectrum of the lanthanum doped-alumina sample shows two peaks one around −3.6 ppm and the another one centered at ca. 35 ppm. The first peak is assigned to aluminum with octahedral symmetry, while the second one is assigned to aluminum in tetrahedral deformed environment, for some authors Al^V [41]. On the other hand, in alumina and ceria doped-alumina samples, only aluminum in octahedral symmetry is observed. The formation of tetrahedral aluminum in the La_2O_3-doped sample is then an additional support that the lanthanum is responsible for the modification of the aluminum environment due to its incorporation and stabilization into the alumina network.

The incorporation of rare earth oxides into alumina network and its effects in acidity are shown in Fig. 3. In general, the doped-aluminas show higher intensity and definition of the Lewis acid sites determined by pyridine absorption spectra as compared with alumina support. The effect of cerium and lanthanum oxides in the developed acidity is probably due to the modification of the aluminum coordination as was inferred from FTIR-pyridine adsorption [35]. FTIR-pyridine adsorption give information about the nature of the sites (Bronsted or Lewis), but it is difficult to obtain quantitative results. Information about the site density and strength can not be obtained.

To confirm the information obtained from the pyridine adsorption, the *iso*-propanol decomposition was carried out (Table 2). Comparable total activities are reported for alumina and doped-aluminas. These results compared with those obtained from pyridine adsorption are then in good agreement. Total activity is related to the total acidity of the sample under study [41]. Fortunately, the selectivity pattern of the *iso*-propanol decomposition gives additional information. The main products obtained from the *iso*-propanol decomposition are: (i) the dehydration product propene, which depends of strong acid sites; (ii) the *iso*-propylether, which depends of medium and weak acid sites and (iii) acetone which is a acid–base reaction, it is formed only if acid and basic sites coexist [42].

The products obtained on alumina were propene and *iso*-propylether, an indication that in alumina there are a large number of medium and weak acid sites [43]. In La_2O_3–Al_2O_3 support, the only product was propene. In this solid, a comparable acidity to that of alumina (same total rate) is obtained, but a different acid site strength is presumed. Finally, the products obtained on CeO_2–Al_2O_3 are propene and acetone. Ceria is considered as a basic oxide, the formation of acetone is indicative that ceria segregation even at 500°C is occurring. The study of the *iso*-propanol decomposition shows that when the sol–gel method is used for the preparation of alumina or doped-alumina, we can obtain a large variety of solids. The use of this method of preparation allows us to make supports or catalysts in which the acidic–basic properties, the

alumina phase, the BET specific area as well as the reactivity can be controlled from the initial conditions of synthesis.

In noble metal-supported catalysts, the metallic surface area is of great importance to have a complete characterization of the catalysts. Platinum area determination in glasses has been reported by hydrogen chemisorption [9]. In doped-alumina containing lanthanum or cerium oxides the specific area of Pd, Rh and Pt has been determined also by hydrogen chemisorption [23,44,45]. However, due to phenomena like spill-over, low metal content and probable metal-support interactions, it has been recommended to determine the metallic area by means of a "structure insensitive reaction". Benzene hydrogenation and cyclohexane dehydrogenation are classified as structure insensitive reactions and they are reported as an indirect determination of the accessible metal area [44,45]. In our catalysts, the activity for the cyclohexane dehydrogenation (metal mono-functional reaction) was used as a comparative parameter for the determination of the metallic surface area. The results of Table 3 show that the activity of Pt/A_2O_3 catalysts is twice of that shown by the doped-alumina catalysts. These results suggest that in the reference catalyst the metal dispersion is higher. The lower metallic surface area of the doped-catalysts can be due to the La_2O_3 and CeO_2 oxides producing one or more of the effects described above, i.e. spill-over, metal support interaction, etc. A comparison between cyclohexane aromatization activity and gas chemisorption has not been carried out for our catalysts. In some attempts, it was difficult to determine the volume of hydrogen chemisorbed. The H_2 uptake was continuous on function of the H_2 pressure. Hence, the extrapolation to the *y*-axis to determine the volume adsorbed by the monolayer was not accomplished. Therefore, the metal particle size was then determined by an independent TEM (transmission electron microscopy) technique. The particle size distribution obtained by TEM for Pt/Al_2O_3, Pt/La_2O_3–Al_2O_3 and Pt/CeO_2–Al_2O_3 catalysts were 1.5, 2.0 and 2.3 nm, respectively, values which can be considered in good agreement with those obtained by determining the activity test in the cyclohexane dehydrogenation (Fig. 6).

The ability of doped lanthanum and cerium alumina sol–gel supports for the bi-functional *n*-heptane dehydrocyclization (one of the reactions in reforming catalysts) was determined for our preparations. The *n*-heptane dehydrocyclization is a reaction which depends of the support acidity and of the metallic surface area [16]. The results of Table 4 show that the reaction is higher in platinum supported in doped-aluminas than in the reference Pt/Al_2O_3 catalyst in spite of its greater metallic dispersion (Table 3). We must then consider that the main factor affecting the activity for the dehydrocyclization reaction is the support acidity.

Form the FTIR spectra shown in Fig. 3, we can conclude that few differences in acidity can be observed between samples. The indirect acidity determined by means of the *iso*-propanol decomposition is then useful on this case. The rate was comparable for the three catalysts, however, the higher selectivity to propene correspond to the Pt/La_2O_3–Al_2O_3 (Table 2). We can expect then for this catalyst a larger selectivity to toluene and selectivities to this product of 50, 38 and 38% for Pt/La_2O_3–Al_2O_3, Pt/CeO_2–Al_2O_3 and Pt/Al_2O_3, respectively, are reported in Table 4. The hydrocarbon reforming reactions occurring in a industrial reactor require of a fine equilibrium between the support acidity and the exposed metallic surface area. An increase in acidity must produce high yields in hydrogenolysis products. Nevertheless, if the metallic phase (metal dispersion) is present in adequate proportion to the acidity, the dehydrocyclization/hydrogenolysis selectivity ratio should be increased. The toluene/C_1–C_4 ratio obtained for the Pt/La_2O_3–Al_2O_3, Pt/CeO_2–Al_2O_3 and Pt/Al_2O_3 catalysts was 2.08, 1.28 and 1.08, respectively. These results support the characterization given to the doped-alumina supports and platinum supported catalysts.

5. Conclusions

In preparing Al_2O_3, La_2O_3–Al_2O_3 and CeO_2–Al_2O_3 supports by the sol–gel method specific surface areas of 572, 459 and 418 m^2/g were obtained on the solids. The FTIR-pyridine adsorption spectra of the supports shows the formation of Lewis sites with comparable intensity. Nevertheless, from the selectivity pattern of the *iso*-propanol decomposition, different acid site strength distribution on the supports is proposed.

Stabilization of the γ-Al_2O_3 phase was obtained in samples annealed up to 1100°C when the support is

La_2O_3 doped-alumina. In CeO_2 doped-alumina, the γ-Al_2O_3 phase was transformed totally in α-Al_2O_3 and cerianite, suggesting in this case the segregation of CeO_2. The insertion of La in the alumina network was inferred from the formation of pentacoordinated (deformed tetrahedral aluminum) Al^V and aluminum with octahedral symmetry.

Using the cyclohexane dehydrogenation as an indirect metallic surface area determination, the Pt/Al_2O_3 catalyst showed the higher dispersion. When the catalysts were evaluated in the bi-functional *n*-heptane aromatization, the Pt/La_2O_3–Al_2O_3 catalyst had the better selectivity to the formation of toluene.

Acknowledgements

We acknowledge the CONACYT and IMP-FIES by the support given to this study.

References

[1] T. Lopez, R. Gomez, in: L.C. Klein (Ed.), Sol–Gel Optics, Kluwer Academic Publishers, Boston, 1994, 345 pp.
[2] T. López, A. Lopez-Gaona, R. Gomez, Langmuir 6 (1990) 1343.
[3] T. Lopez, P. Bosch, M. Asomoza, R. Gomez, J. Catal. 133 (1992) 247.
[4] T. Lopez, L. Herrera, R. Gomez, W. Zou, K. Robinson, R.D. Gonzalez, J. Catal. 136 (1992) 621.
[5] M. Asomoza, T. Lopez, A. Zamalloa, E. Garciafirgueroa, R. Gomez, J. Catal. 138 (1992) 463.
[6] T. Lopez, P. Bosch, J. Navarrete, M. Asomoza, R. Gomez, J. Sol–Gel Sci. Technol. 1 (1994) 193.
[7] G. Carturan, G. Facchin, V. Gottardi, M. Gugliemi, G. Mavacio, J. Non-Cryst. Solids 48 (1982) 219.
[8] G. Carturan, G. Facchin, G. Cocco, S. Enzo, G. Navacio, J. Catal. 76 (1982) 405.
[9] G. Cocco, L. Schifin, G. Strukul, G. Carturan, J. Catal. 65 (1980) 348.
[10] G. Carturan, G. Cocco, L. Schifin, G. Strukul, J. Catal. 65 (980) 359.
[11] M. Asomoza, T. Lopez, R. Gomez, R.D. Gonzalez, Catal. Today 15 (1992) 547.
[12] P. Bosch, T. Lopez, V.H. Lara, R. Gomez, J. Mol. Catal. 80 (1993) 299.
[13] P. Bosch, T. Lopez, M. Asomoza, R. Gomez, M.A. Cauqui, J.M. Rodriguez-Izquierdo, Langmuir 11 (1995) 4328.
[14] R. Gomez, V. Bertin, M.A. Ramirez, T. Zamudio, P. Bosch, T. Lopez, J. Non-Cryst. Solids 147/148 (1992) 748.
[15] R. Gomez, V. Bertin, P. Bosch, T. Lopez, P. Del Angel, I. Schifter, Catal. Lett. 21 (1993) 309.
[16] R. Gomez, V. Bertin, T. Lopez, G. Ferrat, I. Schifter, J. Mol. Catal. 109 (1996) 55.
[17] K. Balakrishman, R.D. Gonzalez, Langmuir 10 (1994) 2487.
[18] L. Guczi, L. Borko, Zs. Koppany, F. Mizukami, Catal. Lett. 54 (1998) 33.
[19] L. Guczi, Z. Schay, G. Srefler, F. Mizukami, J. Mol. Catal. A: Chem. 141 (1999) 177.
[20] R. Gomez, T. Lopez, S. Castillo, R.D. Gonzalez, J. Sol–Gel Sci. Technol. 1 (1994) 205.
[21] S. Castillo, M. Moran-Pineda, R. Gomez, T. Lopez, J. Catal. 172 (1997) 263.
[22] S. Castillo, M. Moran-Pineda, V. Molina, R. Gomez, T. Lopez, Appl. Catal. B: Environ. 15 (1998) 205.
[23] S. Fuentes, N.E. Bogdanchokova, G. Diaz, M. Pedraza, G.C. Sandoval, Catal. Lett. 47 (1997) 27.
[24] P. Reyes, G. Pecchi, T. Lopez, R. Gomez, J.L.G. Fierro, Appl. Catal. B: Environ. 17 (1998) L7.
[25] C.K. Lambert, R.D. Gonzalez, Appl. Catal. A: Gen. 172 (1998) 233.
[26] C.K. Lambert, R.D. Gonzalez, Microporous Mater. 12 (1997) 179.
[27] M. Moran, S. Castillo, T. Lopez, R. Gomez, A. Cordero-Borboa, O. Novaro, Appl. Catal. B: Environ. 21 (1999) 79.
[28] J.A. Wang, A. Morales, X. Bokhimi, O. Novaro, T. Lopez, R. Gomez, Chem. Mater. 11 (1999) 308.
[29] M. May, M. Asomoza, T. Lopez, R. Gomez, Chem. Mater. 9 (1997) 2395.
[30] D. Martin, D. Duprez, J. Phys. Chem. 100 (1996) 9429.
[31] C. Serre, F. Garin, G. Belon, G. Maire, J. Catal. 141 (1993) 1.
[32] C. Serre, F. Garin, G. Belon, G. Maire, J. Catal. 141 (1993) 8.
[33] M. Fernandez-Garcia, E. Gomez-Rebollo, A. Guerrero-Ruiz, J.C. Conesa, J. Soria, J. Catal. 171 (1997) 146.
[34] R.S. Monteiro, F.B. Noronha, L.C. Dieguez, M. Schmal, Appl. Catal. A: Gen. 131 (1995) 89.
[35] C. Monterra, G. Magnacca, J. Chem. Soc., Faraday Trans. 92 (1996) 5111.
[36] A. Vazquez, T. Lopez, R. Gomez, X. Bokhimi, A. Morales, O. Novaro, J. Solid State Chem. 128 (1997) 161.
[37] K. Tadanaga, H. Kobayashi, T. Minami, J. Non-Cryst. Solids 225 (1998) 230.
[38] H. Kobayashi, K. Tadanaga, T. Minami, J. Mater. Chem. 8 (1998) 1241.
[39] J.A. Wang, X. Bokhimi, O. Novaro, T. Lopez, F. Tzompantzi, R. Gomez, J. Navarrete, M.E. Llanos, E. Lopez-Salinas, J. Mol. Catal. A: Chem. 137 (1999) 239.
[40] J. Ward, Zeolite chemistry and catalysis, in: J.A. Rabo (Ed.), Proceedings of the ACS 171, American Chemical Society, Washington, DC, 1976.
[41] J.A. Wang, X Bokhimi, A. Morales, O. Novaro, T. Lopez, R. Gomez, J. Phys. Chem. B 103 (1999) 299.
[42] J.A. Wang, X. Bokhimi, O. Novaro, T. Lopez, R. Gomez, J. Mol. Catal. A: Chem. 145 (1999) 291.
[43] P. Berteau, B. Delmon, J.L. Dallons, A. Van Gysel, Appl. Catal. 70 (1991) 307.
[44] F. Fajardie, J.F. Temepere, G. Djega-Mariadassou, G. Blanchard, J. Catal. 163 (1996) 77.
[45] E. Rogemond, N. Essayem, R. Frety, V. Perichon, M. Primet, F. Mathis, J. Catal. 166 (1997) 229.